FLUOROMETRY OF TURBID AND ABSORBANT SAMPLES AND THE MEMBRANE FLUIDITY OF INTACT ERYTHROCYTES

JOSEF EISINGER AND JORGE FLORES
AT&T Bell Laboratories, Murray Hill, New Jersey 07974

ABSTRACT In employing intrinsic or extrinsic fluorophores in the study of whole cells, or other strongly absorbant and/or scattering samples, the measured fluorescence intensity and polarization is seriously affected by absorption and scattering within the sample cuvet. These artifacts are analyzed and simple protocols are provided for overcoming them. An expression relating attenuation of the observed emission anisotropy to sample turbidity is derived. The validity of the method is confirmed by experiments in which the emission anisotropies and fluorescence yields of membrane probes in intact erythrocytes was measured with precision. It is also shown that the rotational mobility of the membrane probe 1-phenyl-3-(2-naphthyl)-2-pyrazoline is the same for intact erythrocytes and ghosts. These protocols are particularly useful in measuring the intrinsic fluorescence yield ratio for excimeric and monomeric emission of pyrene-containing membrane probes. This provides a method for determining the local lateral mobility of excimeric probes in intact erythrocytes.

INTRODUCTION

There are now available a variety of sensitive fluorescence probes for measuring structural and dynamic features of large biological assemblies, including whole cells, but their exploitation has been hampered by the formidable absorption and scattering artifacts encountered in the quantitative fluorometry of such samples. Reducing the cell titer in order to reduce these effects may have the undesirable consequence of reducing the available fluorescence signal to unacceptable levels.

Similar difficulties attend the measurement of the polarization of light emitted by fluorophores in turbid samples, since both the excitation and emission light is depolarized in passing through such samples. The depolarization of fluorescence resulting from dipole (i.e., molecular) scattering is less severe and was analyzed in detail by Teale (1), while the importance of correcting fluorescence polarization for scattering by large assemblies like erythrocytes was recently discussed by Kutchai et al. (2). Lentz and his collaborators (3) have proposed an approximate correction factor for the emission anisotropy, which is linear with the sample's turbidity, as measured by a spectrophotometer. This is in accord with the theoretical result derived by Teale (1) and is consistent with the analysis presented here, but because the fluorometer's photodetector generally has a different (and usually unknown) acceptance angle from the absorption spectrophotometer, a concentration-based correction, like the one proposed here, is more accurate and is easier to use in experiments.

Here we investigate, theoretically and experimentally, how the fluorescence intensity and polarization, as measured in a conventional right angle fluorometer, depends on the absorption and scattering characteristics of the particles and on their concentration (titer) in the sample. This analysis leads to simple protocols for determining the intrinsic fluorescence yield and polarization of the light emitted by fluorophores in turbid and absorbant samples. The validity of these protocols is confirmed by the quantitative fluorometry and polarimetry of suspensions of red blood cells (RBCs) with hematocrits of up to 0.5%. These methods are employed in a comparison of the rotational diffusion of membrane probes in intact cells and ghosts. They are also shown to be useful in the determination of the intrinsic intensity ratio of excimeric and monomeric emission of a pyrene-containing membrane probe. It is shown elsewhere how this ratio may be used to determine the local lateral fluidity of membranes of intact erythrocytes (4, 5; Eisinger, J., J. Flores, and W. S. Petersen, manuscript in preparation).

METHODS

Blood was drawn from normal, casual donors and was used in experiments within 2 d. Erythrocytes were washed three times before probes were inserted into their membranes. They were washed and their fluorescence was measured in a buffer (BSG) containing 10 mM Na-phosphate, 0.15 M NaCl, and 2 g/l of glucose, adjusted to pH 7.4.

1-pyrenedodecanoic acid (PDA) (Molecular Probes, Junction City, OR) was dissolved in tetrahydrofuran (THF) and was subsequently added to ethanol (~5 mg/ml ethanol, 10% THF) to make a stock solution whose precise molarity was determined by absorption spectroscopy, using $\epsilon(\text{mM}) = 40\ \text{cm}^{-1}$ at 345 nm. To label erythrocytes, 0.5 to 10 μl of this stock solution per milliliter of packed RBC were added to red cell suspensions at a hematocrit of 0.2. The cells were incubated for 30 min at 20°C and were then washed three times with BSG. The data of Fig. 1

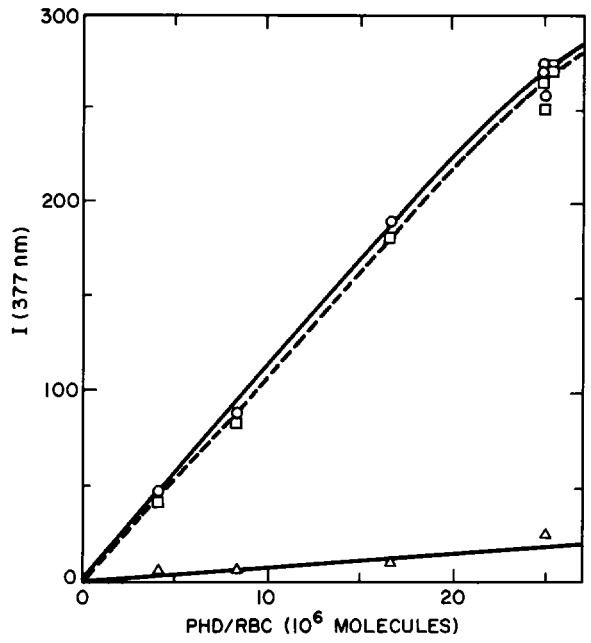

FIGURE 1 The PDA fluorescence intensity measured at 377 nm by front face fluorescence at a hematocrit of 16% following the addition of 1% SDS to lyse erythrocytes. Since PDA is incorporated into SDS micelles I (377 nm) is, for the probe ratios employed here, a measure of the number of PDA molecules present in the sample. Note that virtually all probes added to an RBC suspension (O) are retained by the cells following three centrifugations and washings (□) and that the fraction in the supernatant after osmotic lysis and pelleting of ghost membranes is <10% (Δ).

show that when PDA probes are added to a suspension of intact RBC, virtually all probes are taken up by the cells and remain in the cells' membranes after two washings: After osmotic lysis and sedimentation of the ghosts by centrifugation, <5% of the probes are found to remain in the supernatant. The number of probes in washed ghosts (n_G) was determined spectrophotometrically following the addition of 1% of sodium dodecanyl sulfonate (SDS) and was found to be smaller than the number per intact cell (n_R) by 10–40%. n_R was taken to be the number of probes added to the cell suspension. Ghost titres were obtained from the absorbance at 280 nm, following the addition of 1% SDS to reduce scattering effects, with one absorbance unit corresponding to a ghost titre of 2.15×10^9 ml^{-1} (6). Allowance was made for the contribution of PDA absorbance at 280 nm using A(280 nm) = 0.067 A(344 nm). The titres of intact cells were determined from the dilution of suspensions of known hematocrit assuming 1.15×10^{10} ml^{-1} for packed cells.

1,6-diphenylhexatriene (DPH) or 1-phenyl-3-(2-naphthyl)-2-pyrazoline (PNP) probes were inserted into the membranes of intact erythrocytes by incubating them for 30 min at room temperature at a hematocrit of 0.25%. The incubation mixture was made by adding 25 μl of DPH or PNP stock solutions (~0.04 mg/ml ethanol) to 25 ml of BSG buffer containing RBCs at a hematocrit of 0.25%.

Steady state fluorescence intensity and polarization measurements were performed by means of a modified SLM spectrofluorometer (SLM Instruments, Champaign, IL) and fluorescence decay rates were determined by a monophoton time correlation system, using instrumentation described elsewhere (6). Absorption spectra were measured by means of a Cary 17 spectrophotometer (Varian Associates, Inc., Palo Alto, CA). 3 mm × 3 mm quartz cuvettes were used for all fluorescence measurements (Precision Cells, Hicksville, NY). With these cells the absorption and scattering artifacts are smaller and the observed emission intensity is larger than in the commonly used 1-cm cuvettes (7).

THEORY

We investigate how the intrinsic fluorescence intensity and polarization of fluorophores in a sample are affected by the scattering and absorption of excitation and emitted light within the cuvette. In the present study the fluorophores are attached to the scattering and absorbant particles (cells) and it is assumed that these are randomly distributed in the cuvette. However, this association between scatters and fluorophores is in general not necessary.

Fluorescence Intensity

In a conventional spectrofluorometer employing a nonscattering sample, the excitation light is focused at the center of a square cross section cuvette as indicated in Fig. 2. The fluorescence emitted within a certain solid angle at right angles to the excitation beam direction is collected by the emission optical systems and is eventually measured by a suitable photodetector. In considering the absorption and scattering effects within the cuvette we follow a beam of excitation light into the central region of the cuvette which is considered optically active because it is common to both the excitation and emission optics. This region is heavily stipled in the schematic representation of Fig. 2.

The fractional intensity lost by light traveling along the z direction through an infinitesimal slab (thickness dz) of a sample containing absorbant and scattering particles is proportional to the concentration of scatterers, h, and to dz:

$$dI/I = -(\alpha_a + \alpha_s)\, h\, dz, \qquad (1)$$

where α_a and α_s a the wavelength dependent attenuation coefficients due to absorption and scattering through a sufficiently large angle to remove photons from the beam. If the pathlength of the excitation light (I_{ex}) within the cuvette is z, its intensity in the cuvette is obtained by

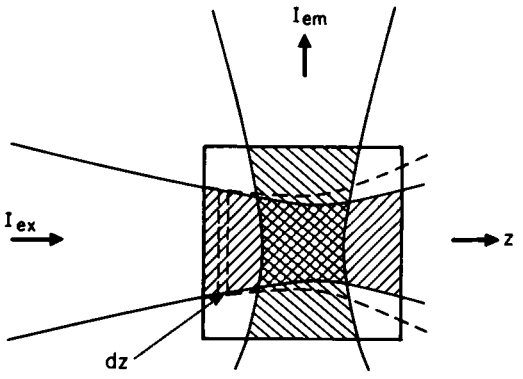

FIGURE 2 A schematic representation of the excitation and emission beams (shown stipled) in a right-angle fluorometer. The volume element that is common to them, the optically active region, is heavily stipled. If the sample scatters light, the excitation beam is broadened as indicated by the dashed lines.

integration of Eq. 2

$$I(z) = I_{ex} \exp [(-\alpha_a - \alpha_s)\, hz]. \quad (2)$$

If each scattering and/or absorbing particle in the sample contains n fluorophores with quantum yield ϕ, the fluorescence intensity reaching the detector can therefore be written

$$I = CI_{ex} nh\phi e^{-\alpha h}, \quad (3)$$

where α is the lumped attenuation coefficient for absorption and scattering losses in both the exciting and fluorescence light, which is attenuated analogously to Eq. 2. α is therefore a function of the excitation and emission wavelengths (λ_{ex}, λ_{em}) and of the effective pathlengths of the excitation and fluorescence beams and where C is an instrumental constant. Eq. 3 may be rewritten in logarithmic form as

$$\ln (I/h) = \ln J - \alpha h. \quad (4)$$

According to Eq. 4, a semilogarithmic plot of the relative fluorescence yield I/h vs. h is a straight line whose intercept, J, is proportional to $n\phi$, the number and quantum yield of the fluorophores, and whose slope is $-\alpha$.

The exponential dependence of I/h on h predicted by Eq. 4 is valid below a certain concentration, which depends on scattering properties (cross section and angular distribution) of the particles and on the configuration of the fluorometer. This can be seen by considering the effect of twice-scattered photons, particularly back-scattered ones: for at sufficiently great concentrations these are not permanently lost from the beam and the coefficient α_s is no longer independent of h. The concentration range for which Eq. 3 remains valid therefore depends on the angular distribution of the scattered light, the dimensions of the cuvette and the fluorometer optics. Since the scattering characteristics of irregularly shaped and absorbant particles are extremely complex (8), the range of validity of Eq. 4 is best best determined empirically and is expected to be greatest where α is small and when the scattered light is strongly peaked in the forward direction.[1] It will be seen below that the linear relationship of Eq. 4 is confirmed by experiment for RBCs with hematocrits of $\lesssim 1\%$.

Fluorescence Depolarization of Turbid Samples

Consider a beam of light traveling along the z direction through a turbid medium (Fig. 2). The state of polarization of the light is characterized by its anisotropy r, defined by

$$r(z) = \frac{I_v(z) - I_h(z)}{I_t(z)}, \quad (5)$$

where $I_v(z)$ and $I_h(z)$ are the vertical and horizontally polarized intensities and the total intensity is $I_t(z) = I_v(z) + 2I_h(z)$. In passing through an infinitesimal slab (thickness dz) of randomly distributed scatterers (concentration h) the fraction of vertically polarized light that is converted to horizontally polarized light is the same as the fraction of horizontally polarized light that becomes vertically polarized, both fractions (δ) being proportional to h and dz. Therefore,

$$I_v(z + dz) = I_v(z)\,(1 - \delta) + I_h(z)\delta \quad (6a)$$

and

$$I_h(z + dz) = I_h(z)\,(1 - \delta) + I_v(z)\delta, \quad (6b)$$

where we have for convenience written $\delta = \frac{1}{2}\beta' h dz$, β' being a wavelength-dependent constant, which is characteristic of the scattering particles. By using Eq. 6 in Eq. 5 and making use of $\delta \ll 1$,

$$r(z + dz) = r(z)\,[1 - 2\delta - r(z)\delta] \quad (7)$$

so that

$$\frac{dr}{r(z)[2 + r(z)]} = -\beta' h dz. \quad (8)$$

Eq. 8 is readily integrated from $r(0)$, the anisotropy of the light entering the sample, to $r(z)$ and becomes

$$\ln \frac{r(z)}{r(0)} - \ln \frac{2 + r(z)}{2 + r(0)} = -\frac{1}{2}\beta' hz. \quad (9)$$

Eq. 9 shows how the anisotropy of polarized light is reduced in passing through a scattering medium. For the purposes of the present analysis the equation may be simplified by noting that in the absence of the second term on the left side, r would decrease exponentially with h and z. The contribution of the second term is greatest when $r(0) = 1$, i.e., for linearly polarized light, and it is easily shown that even for this worst case, the left side of Eq. 9 is linear with z as long as $r(z)/r(0) \gtrsim 0.7$. In this domain Eq. 9 may therefore be formally replaced by

$$r(z) = r(0)e^{-\beta hz}, \quad (10)$$

where it is understood that anisotropy decrease while passing through the sample does not exceed ~30%. In terms of the so-called depolarization factor, $d(z) = r(z)/r(0)$, therefore,

$$d(z) = e^{-\beta hz}. \quad (11)$$

Note that according to Eq. 9–11, the fractional anisotropy decrement due to scattering is very nearly linear with the

[1]This is clearly the case for human erythrocytes for which the scattered light (450 nm) has an angular spread of ~20° for a pathlength of 1 mm at a hematocrit of 0.25% (Blumberg, W. E., J. Eisinger, and J. Flores, unpublished results).

samples turbidity (absorbance), in agreement with Teale's theoretical and experimental results (1).

Consider a sample that contains scattering particles and intrinsic (or extrinsic) fluorophores, whose emission anisotropy is r_f. If the excitation light is vertically polarized, (i.e., $r[0] = 1$), the observed emission anisotropy is according to Solleilet's theorem (9)

$$r = d_{ex} r_f d_{em} \tag{12}$$

where d_{ex} and d_{em} are the depolarization factors for the depolarizations suffered by the excitation and emitted light, respectively. Using Eq. 11 in Eq. 12 and taking logarithms, the observed anisotrophy, r, is therefore given by

$$\ln r = \ln r_f - \gamma h, \tag{13}$$

where γ is the lumped anisotropy attenuation coefficient that depends on λ_{ex} and λ_{em} and on the effective pathlengths of the excitation and emitted light in the sample cell. It follows from Eq. 13, that a semilogarithmic plot of the measured (apparent) values of r vs. h is a straight line with a negative slope γ, whose intercept gives the true anisotropy of the fluorophores, r_f.

Note that for a sample with sufficiently low turbidity and an effective absorbance A, Eq. 10 approaches the expression suggested by Lentz et al. (3)

$$r(z) = r(0)(1 - KA), \tag{14}$$

where K is a constant.

Lateral Mobility and Excimer Formation

It is well known that an excited pyrene molecule in close proximity to one in its ground state may form a dimer in an excited singlet state ("excimer") (10). The fluorescence emitted by the excimer is broad, unstructured, and red-shifted with respect to the monomer emission and is therefore readily distinguishable and well resolved from it. Since an excimer can form only if the excited pyrene molecule becomes a nearest neighbor to one in its ground state in a time comparable to the excited state lifetime, the relative yields of excimeric and monomeric fluorescence from a pyrene-containing lipid analogue (e.g., PDA) is a measure of the probe's lateral mobility within the membrane (4, 5). While this method of determining the local lateral fluidity has been employed in various model membrane systems, including vesicles and erythrocyte ghosts, no attempts to employ it with intact cells have been reported. A detailed analysis of how the excimer production rate is related to the lateral mobility and to the probe/lipid ratio is presented elsewhere (Eisinger, J., J. Flores, and W. S. Peterson, manuscript in preparation). Here we are only concerned with the determination of the intrinsic excimer/monomer yield ratio, the experimental parameter from which the probe's lateral mobility is derived by the use of a suitable model (Eisinger, J., J. Flores, and W. S. Petersen, manuscript in preparation).

Let $I_M(h)$ and $I_E(h)$ be the observed fluorescence intensities at the maxima for the monomeric (377 nm) and excimeric (479 nm) emission spectra of the probe (PDA), embedded in the membranes of a suspension of RBC with a hematocrit h. The intensity and quantum yield ratios for excimeric and monomeric emissions are related by

$$I_E(h)/I_M(h) = \kappa(\phi_E/\phi_M), \tag{15}$$

where the constant κ is readily determined from the integrated monomeric and excimeric emission spectra. It follows from Eq. 3, after cancellation of C, I_{ex}, n, and h that the ratio

$$\rho(h) \equiv \frac{I_E(h)}{I_M(h)} = \kappa \frac{\phi_E}{\phi_M} \exp\left[(\alpha_M - \alpha_E)h\right] \tag{16}$$

or

$$\rho(h) = \rho_0 \exp\left[(\alpha_M - \alpha_E)h\right], \tag{17}$$

where α_M and α_E are the effective attenuation coefficients for monomeric and excimeric fluorescence and ρ_0 is the true excimeric /monomeric intensity ratio for vanishingly small h. A semilogarithmic plot of $\rho(h)$ vs. h should accordingly be a straight line with slope $\alpha_M - \alpha_E$, whose intercept is equal to ρ_0.

EXPERIMENTAL RESULTS

Washed erythrocytes were labeled with the lipid analogue, PDA, and the pyrene fluorescence yield was measured in a series of samples whose hematocrits ranged up to 5×10^{-3}. The excimer intensity measured at its maximum (479 nm) was corrected for a small contribution at that wavelength from the tail of the monomer spectrum, the correction being $-0.01\ I_M$, where I_M is the monomer intensity at its spectral maximum at 377 nm. Both I_M and I_E were also corrected for a very small background intensity, which was determined for a sample containing the same erythrocytes at the same hematocrit but without probes. The monomer and excimer intensities and their ratio are shown as a function of the hematocrit, h, in Fig. 3 *a*. $I_M(h)$ initially increases with hematocrit, reaching a maximum at $h \approx 3 \times 10^{-3}$, before declining because of the increasing absorption and scattering losses within the sample cell.

Fig. 3 *b* shows the same data as a semilogarithmic plot of the monomeric and excimeric yields vs. h and it can be seen that the linear relationship predicted by Eq. 4 is valid for both $I_M(h)/h$ and $I_E(h)/h$. The effective attenuation coefficients, α(377 nm) and α(479 nm) are obtained from the slopes of these lines and are listed, along with the intercepts at $h = 0$, J_M and J_E, in Table I.

Two other approaches for measuring relative fluorescence yields in highly scattering and absorbant samples have been employed in the past. These are front face fluorometry (7) and the summed intensity contributions of

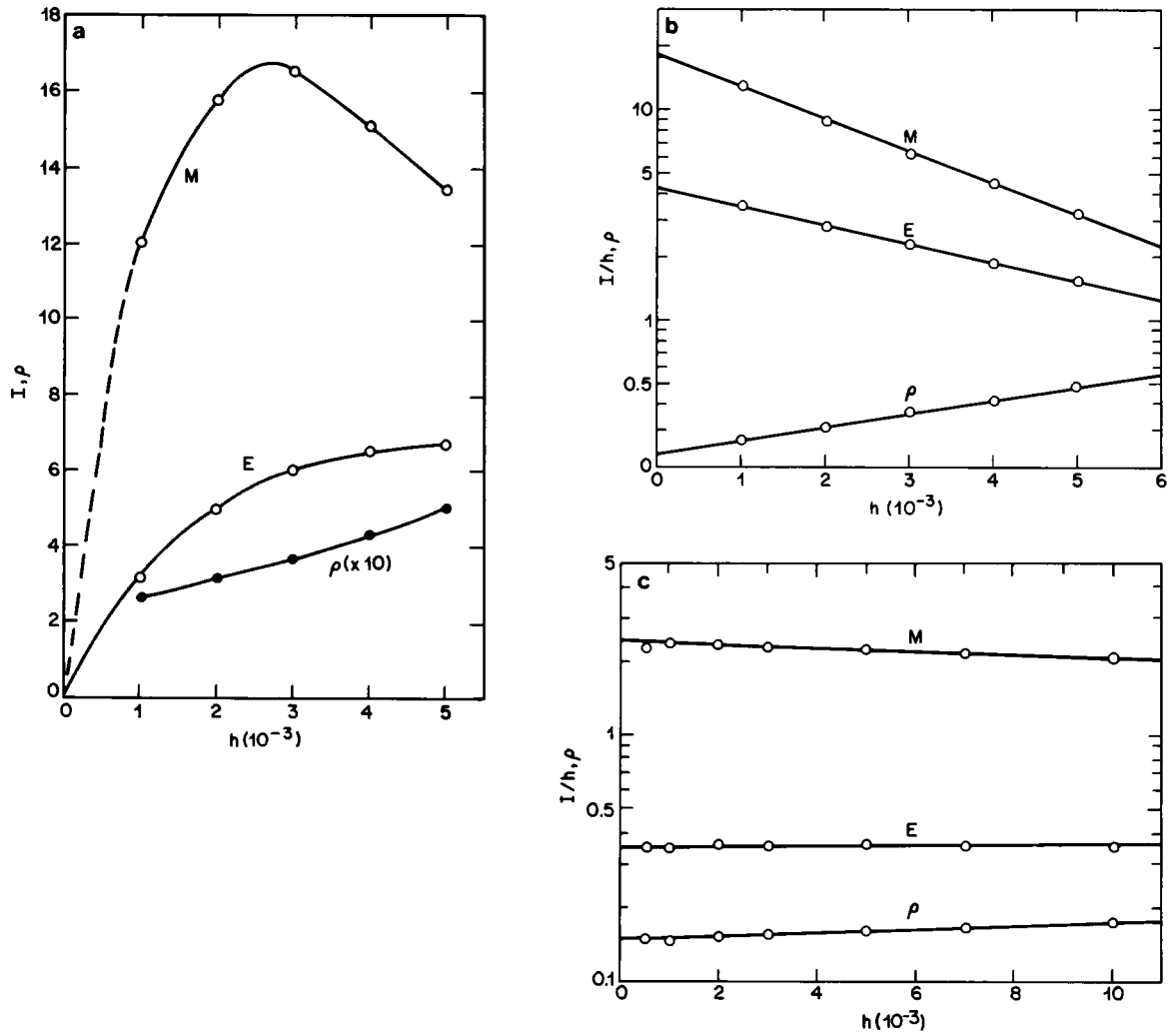

FIGURE 3 (*a*) The monomeric (*M*) and excimeric (*E*) fluorescence intensities at 21°C of PDA embedded in intact erythrocytes, and their ratio, ρ, as function of the sample hematocrit, *h*. (*b*) The same data plotted semilogarithmically (as yields, I/h) are seen to fall on straight lines, in accordance with Eqs. 4 and 17, with a larger negative slope (α) for the monomer than for the excimer yield, because the former is measured at 377 nm where erythrocytes absorb and scatter light more strongly than at 479 nm. (*c*) After lysis of the PDA-labeled cells and removal of the cytoplasm by centrifugation the fluorescence of the PDA-labeled ghosts were measured and plotted as in *b*. Note that because ghosts scatter and absorb light much less than intact erythrocytes, the slopes of the straight lines are considerably smaller.

the fluorophore's decay components (4), i.e., $I_D = \Sigma\, \alpha_i\, \tau_i$, where α_i and τ_i are the amplitude and decay time of the *i*th component of the fluorescence decay. We measured the relative monomer intensities for PDA labeled RBC by these two methods and compared their ratios for three different osmotic strengths to the relative values (J) obtained by the h extrapolation protocol (cf., Eq. 4). The membrane probes' yield decreases as the osmotic strength of the buffer is raised because this causes the cells to shrink and because the increased hemoglobin concentration in the cytosol boundary layer increases the resonance energy transfer rate from the probes in the membrane to the hemes (6). The last three columns of Table I give the monomeric intensities at 195 and 401 mOsM osmotic strengths relative to the physiological one (290 mOsM), as measured by these three methods. Front face intensities (I_{FF}) were obtained at a hematocrit of 0.25, as were the decay rate intensities (I_D). It is seen that the relative values of I_{FF} and I_D agree with the relative J_M values within experimental uncertainties. The attenuation coefficients α(377 nm) and α(479 nm), indicative of the cells' absorbance and scattering properties, are given in inverse hematocrit units and are seen to be the same at 195 and 290 mOsM, but somewhat higher at 402 mOsM. At 402 mOsM the erythrocytes' shrinkage becomes significant and appears to affect their scattering properties slightly.

According to Eq. 17, the slope of a logarithmic plot of $\rho(h)$ vs. h should be $\alpha_M - \alpha_E$, where α_M and α_E are the slopes obtained from semilogarithmic plots of I_M/h and I_E/h, respectively. A comparison of columns 6, 7, and 8 of Table I shows this to be the case within the experimental uncertainties, at all three ionic strengths investigated.

TABLE I
COMPARISON OF FLUORESCENCE PARAMETERS OF PDA-LABELED ERYTHROCYTES MEASURED AT THREE OSMOTIC STRENGTHS

OS*	J_M	J_E	J_E/J_M	ρ_0‡	$\alpha(377)$	$\alpha(479)$	$\frac{1}{\rho}\frac{d\rho}{dh}$‡	$\frac{J_M(OS)}{J_M(290)}$	$\frac{I_{FF}(OS)}{I_{FF}(290)}$	$\frac{I_D(OS)}{I_D(290)}$
mOsM										
195	21.6	5.2	0.241	0.233	347	204	153	1.19	1.18	1.17
290	18.2	4.25	0.233	0.230	345	203	149	(1.00)	(1.00)	(1.00)
402	17.0	4.0	0.235	0.228	372	222	160	0.93	0.92	0.89
$\pm\sigma$:§	0.5	0.1	0.01	0.005	7	7	10	0.03	0.03	0.05

The table gives the corrected monomer and excimer fluorescence yields (J_M, J_E) in arbitrary units of PDA in the membranes of intact erythrocytes obtained by extrapolation to zero hematocrit according to Eq. 4. Data are given for three osmotic strengths. The fourth column gives the values of J_E/J_M that are seen to agree with ρ_0, the value of $\rho(h)$ extrapolated to zero hematocrit. Columns 6 and 7 give α (377 nm) and α(479 nm), the effective extinction coefficients at the monomer and excimer wavelengths (cf. Eq. 4). The difference between them is seen to be equal to the slope $d(\ln \rho)/dh$ given in column 8 (cf. Eq. 17). Columns 9 and 10 give the monomeric fluorescence intensities at low (195 mOsM) and high (402 mOsM) osmotic strengths, relative to the physiological one (290 mOsM), as measured by J_M, front face fluorometry (I_{FF}), and fluorescence decay rate (I_D), respectively.

*Osmotic strength.

‡See Eqs. 22 and 23.

§Experimental standard deviations.

Within experimental errors, the corrected excimer/monomer yield ratios J_E/J_M (or ρ_0) are independent of ionic strength, which shows the dynamic properties of the membrane, (i.e., the local lateral fluidity) are not very sensitive to the ionic conditions. The data of Table I were obtained with RBC for which n_R, the number of PDA probes per cell, was 2.1×10^7. This corresponds to a probe to phospholipid ratio of ~10%, if the number of lipids (including cholesterol) per membrane leaflet is taken to be 2.2×10^8 per cell. The dependence of ρ_0 on the probe ratio is reported elsewhere (Eisinger, J., J. Flores, W. S. Petersen, manuscript in preparation) as is a model with which the probe-phospholipid exchange frequency, and the local lateral diffusion constant, which may be extracted from these experiments.

Polarization Measurements

The steady state fluorescence polarization of a membrane probe has long been recognized as being indicative of the membrane's fluidity (11). The most widely used reorientational probe is DPH, which emits at ~400 nm, but PNP, a similar hydrophobic membrane probe offers important advantages, such as lower photolability and a longer emission wavelength (~500 nm), where the attenuation due to the red cells' absorption and scattering is smaller (12).

Figs. 4 and 5 show semilogarithmic yield titrations for DPH- and PNP-labeled intact erythrocytes, at hematocrits ranging up to 2–3%. It can be seen that over this range the yield and anisotropy dependence on h is as predicted by Eq. 4. The slope, α, in inverse hematocrit units is −2,060 and −700 for DPH and PNP, respectively, which is consistent with the considerations of the preceding paragraph.

Fig. 5 also compares yield data for erythrocytes and ghosts made by osmotic lysis. Because both absorption and

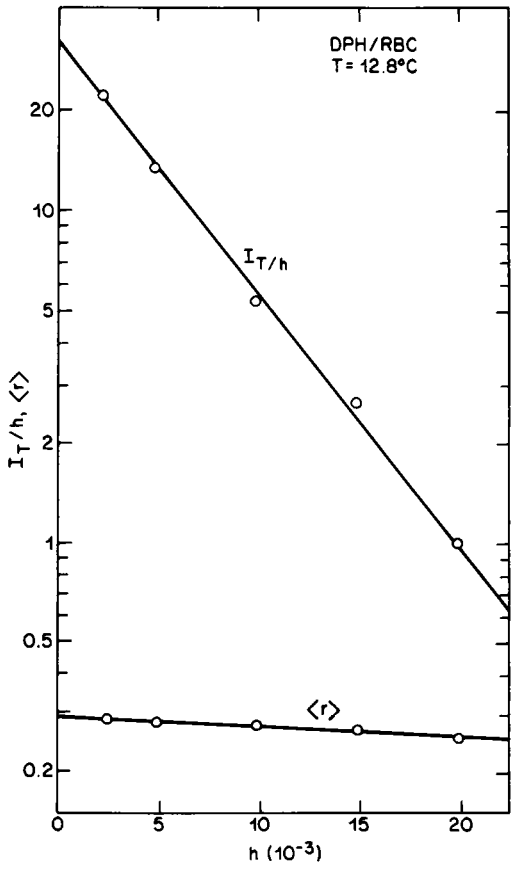

FIGURE 4 Semilogarithmic plots of the total yield, I_T/h, and steady state emission anisotropy, $\langle r \rangle$, of DPH-labeled intact cells at 12.8°C as a function of hematocrit. The excitation and emission wavelengths were 355 and 460 nm, respectively.

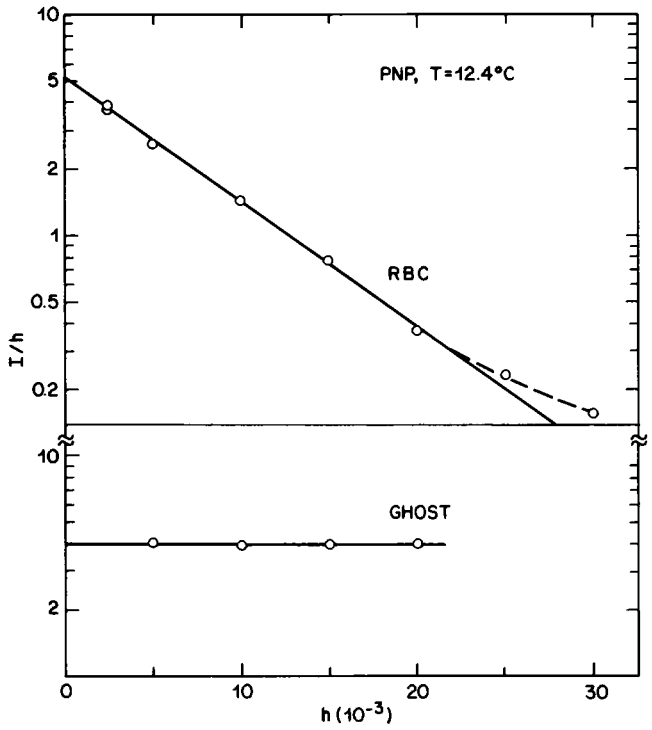

FIGURE 5 Semilogarithmic plots of the yield of PNP embedded in intact RBC and in ghosts at 12.4°C. Note that the slope (α in Eq. 3) is smaller for PNP than for DPH because the emission wavelength is longer.

scattering are greatly reduced, the slope α is vanishingly small for ghosts. We finally compared the extrapolated steady state emission anisotropies of PNP in ghosts and in intact erythrocytes at 12°C (Fig. 6 *a*) and obtain values of 0.259 ± 0.05 and 0.272 ± 0.005, respectively. This difference in anisotropies is because of experimental errors, only of marginal significance, but suggests that lysis increases the rotational fluidity of the erythrocyte's membrane slightly. Note, however, that for the intact cell the fluorescence lifetime is expected to be a few percent shorter, because of energy transfer to hemoglobin, and this would increase the observed anisotropy of PNP in intact RBC slightly. In any case, the intact cell's membrane is, contrary to a previous suggestion (13), no more fluid than that of its ghost at any temperature (Fig. 6 *b*) and is somewhat less fluid at high temperatures, where ghosts tend to vesiculate.

DISCUSSION

We have described a simple new protocol for correcting the measured emission anisotropy of turbid samples and have tested it by investigating samples of erythrocytes labeled with two fluorophores. In a study of PNP-labeled intact erythrocytes and ghosts it was concluded that the probe's anisotropy is very nearly the same in both systems. This is at variance with the conclusion based on uncorrected polarization measurements that the membrane fluidity of intact RBC is 50% greater than for ghosts (13).

Kutchai et al. (2) used a linear concentration extrapolation of his experimental DPH anisotropies at 37°C to obtain a correct $\langle r \rangle = 0.16$ and 0.22 for intact erythrocytes and ghosts, respectively. This difference in the apparent membrane fluidity in cells and ghosts is probably due to the high cell titre employed by these investigators (hematocrit between 1 and 11%), particularly if the measurements were made in a 1 cm × 1 cm cuvette.

In summary, we have described a simple fluorometric titration method with which the relative yield and emission anisotropy of fluorophores in absorbant and turbid samples may be determined with precision. It is of course applicable to systems other than suspensions of erythrocytes and ghosts. The range of applicability of the protocol for particular system is readily tested: If one obtains a straight

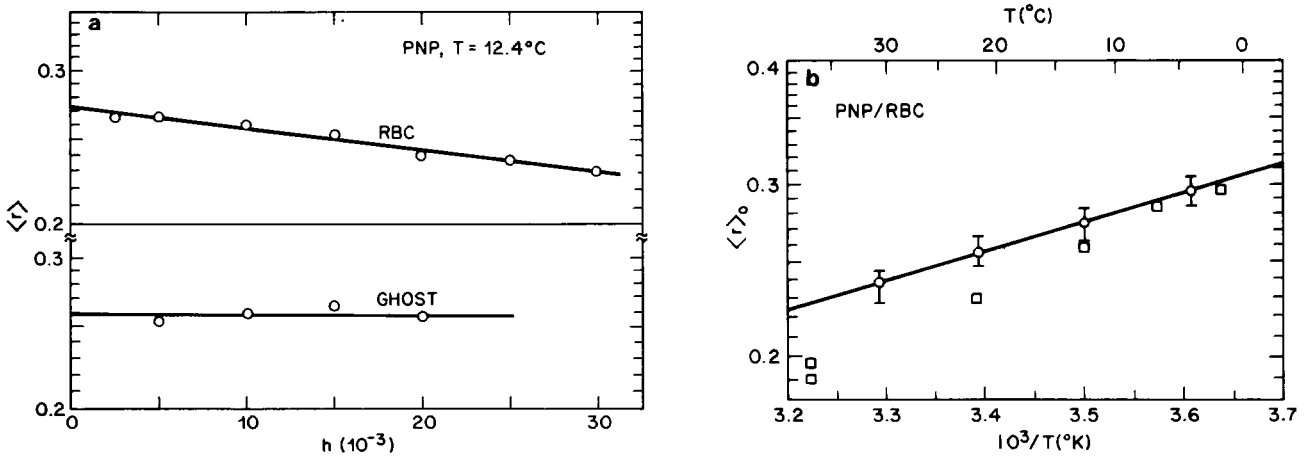

FIGURE 6 (*a*) Semilogarithmic plot of the concentration-dependent steady state emission anisotrophy of PNP in intact erythrocytes and ghosts at 12.4°C. The intercept at $h = 0$ gives $\langle r \rangle_0$, the corrected emission anisotropy. (*b*) The temperature dependence of the corrected emission anisotropy $\langle r \rangle_0$ of PNP in erythrocyte membranes (O), obtained as in *a*. Also shown are corrected values of $\langle r \rangle_0$ for ghosts (□) that are the same as for intact cells at low temperature but somewhat lower at temperatures above 15°C.

line by plotting log (I/h) vs. h, the assumption of Eq. 4 are satisfied and the semilogarithmic extrapolation provides the appropriate correction. This protocol is particularly useful for the determination of the intrinsic excimer/monomer yield ratio of excimeric membrane probes and can therefore be used to determine the local fluidity of membranes of intact cells (Eisinger, J., J. Flores, and W. S. Petersen, manuscript in preparation).

We thank F. J. Doleiden and Abraham Hsuan for valuable technical help.

Received for publication 10 September 1984 and in final form 1 February 1985.

REFERENCES

1. Teale, F. W. J. 1969. Fluorescence depolarization by light-scattering in turbid solutions. *Photochem. Photobiol.* 10:363–374.
2. Kutchai, H., V. H. Huxley, and L. H. Chandler. 1982. Determination of fluorescence polarization of membrane probes in intact erythrocytes. *Biophys. J.* 39:229–232.
3. Lentz, B. R., B. M. Moore, and D. A. Barrow. 1979. Light scattering effects in the measurement of membrane microviscosity with diphenylhexatriene. *Biophys. J.* 25:489–494.
4. Galla, H.-J., and E. Sackmann. 1974. Lateral diffusion in the hydrophobic region of membranes. Use of pyrene excimers as optical probes. *Biochim. Biophys. Acta.* 339:103–115.
5. Galla, H.-J., and W. Hartmann. 1980. Excimer—forming lipids in membrane research. *Chem. Phys. Lipids.* 27:199–219.
6. Eisinger, J., and J. Flores. 1983. Cytosol-membrane interface of human erythrocytes. *Biophys. J.* 41:367–379.
7. Eisinger, J., and J. Flores. 1979. Front face fluorometry of liquid samples. *Anal. Biochem.* 94:15–21.
8. Van de Hulst, H. C. 1957. Light Scattering by Small Particles. John Wiley & Sons, Inc., New York.
9. Solleilet, P. 1929. Sur les paramétres caractérisant la polarization partielle de la lumière dans les phénomènes de fluorescence. *Ann. Phys. (Paris).* 12:23–97.
10. Förster, Th., and H.-P. Seidel. 1965. Untersuchungen zum Konzentrationsumschlag der Fluoreszenz des Pyrens. *Z. Phys. Chem.* 45:58–71.
11. Shinitzky, M., A.-C Dianoux, C. Gitler, and G. Weber. 1971. Microviscosity and order in the hydrocarbon region of micelles and membranes determined with fluorescent probes. I. Synthetic micelles. *Biochemistry.* 10:2106–2112.
12. Eisinger, J., N. Boens, and J. Flores. 1981. Fluorescence polarization studies of human erythrocyte membranes with 1-phenyl-3-(2-naphthyl)-2-pyrazoline as orientational probe. *Biochim. Biophys. Acta.* 646:334–343.
13. Aloni, B., M. Shinitzky, and A. Livne. 1974. Dynamics of erythrocyte lipids in intact cells, in ghost membranes and in liposomes. *Biochem. Biophys. Acta.* 348:438–441.